Egyptian Journal of Chemistry

http://ejchem.journals.ekb.eg/

Effect of Variation in Polymer Structure on Eddies Suppression of Basrah Light Crude Oil Turbulent Flow

Mahir A. Jalal[a]*, Moayad N. Khalaf[b], Mouayed A. Hussein[b]

[a] *Department of Polymer Technology, Polymer Research Center, University of Basrah, Basrah 61001, Iraq*
[b] *Department of Chemistry, College of Science, University of Basrah, Basrah 61001, Iraq*

Abstract

Poly(pentaerythritol adipate), poly(pentaerythritol sebacate), and poly(pentaerythritol hexadecandioate) derivatives containing different length alkyl branches were synthesized by two subsequent steps; the reaction of pentaerythritol with (C8-C16) linear aliphatic monocarboxylic acids and then, polymerization of products with (C_6-C_{16}) linear aliphatic dicarboxylic acids, using 1% para toluene sulfonic acid as a catalyst. The products were purified and characterized by FTIR, ^{1}H NMR, and ^{13}C NMR spectroscopy. End group analysis was also used as a molecular weight determination technique. The drag-reducing properties of those polymers were investigated in the turbulent flow of Basrah light crude oil using a closed-loop circulation system. Some were found to perform very well DRA and drag reduction efficacy of polymer was further found to be dependent on flowrate, polymer concentration, medium-temperature, and its chemical structure. Also, the effect of the imposed mechanical shear on the polymer stability as a function of time has been investigated using a cylindrical rotator device. It was observed that distance between branch points plays a direct role in contributing to the polymer performance and its mechanical stability.

1. Introduction

The transfer of the crude oil through the pipeline technology is very important to the world economy. In the last decades, strong global consumption growth in crude oil poses challenges for oil transportation in which pipeline upgrading is considerably expensive and doubling pumped energy will not lead to double the flow rate due to the fact of increasing turbulence in the flow and, consequently, increase in the amount of flow energy loss. These challenges were received special interest from of researchers for finding approaches can address oil global production shortfall. Thus, the drag-reducing agents (DRA) are implemented to reduce the pressure drop, when the flow is turbulent, and increase the amount of oil production. Such implementation significantly reflects their economic benefits on the petroleum industry [1].

The observation of the drag reduction phenomenon was first raised in 1948 by Tom [2] who found that

adding low concentrations of PMM polymer can improve the drag reduction up to 40%. However, the breakthrough of bringing DRA in practical implementation was started in the Trans-Alaskan pipeline in 1979, by adding polymer-oil soluble of 10% of CDR solution [3]. Researches were continued and several of them have been recently conducted for using polymeric DRA in improving crude oil and other types of solvents flow. Rabeeah et al [4] found 50 ppm of polystyrene and polydimethylsiloxane can reduce the pressure drop of the crude oil up to 29% and 25%, respectively. Cole et al [5] synthesized some architecture polymers using atom transfer radical polymerization (ATRP), tested them as DRAs in aqueous media using ring test, and found that some of them can exhibit a comparable level of performance with PAA. Xing et al [6] revealed that introducing Nanosilica to the structure of copolymer of sodium 4-styrene sulfonate, acrylamide,

_____

dimethylhexadeylallylammonium bromide can enhance the degree of drag reduction performance and mechanical shear stability. Others [7] synthesized associating terpolymers of polyethylene glycol, acrylic acid, and acrylamide and found the low doses of the copolymer, as low as 23 ppm, demonstrate high drag reduction percentages up to 76% in water. Guoyan et al [8] found that polymers of acylamide, 2-acrylamide-2-methylpropane sulfonic, acrylic acid and dodecyl 2-methyl acrylate showed a high level of drag reduction, 62.38%, due to the formation of hydrophobic intermolecular associations. Studies were also extended to employ the synergetic effect of polymeric DRA with other polymeric or non-polymeric species in improving flow characteristics. Huang [9] pointed that an inter-entangled network of polymers existed when using the solutions of polyethylene oxide and carboxymethyl cellulose which exhibits some improvement in reducing pressure drop. Arthurs [10] exploited an interaction between anionic copolymer of poly(acrylamide-co-diallyl dimethylammonium chloride) and nonionic surfactant (tween 20) for producing better DRA performance and mechanical stability in aqueous media. Dia et al [11] pointed out using a mixture of non-ionic polyolefins, cetyl trimethyl ammonium bromide as a cationic surfactant, and salt of sodium salicylate as its counter-ion in diesel can reduce the pressure drop to 40%.

Several types of research have been conducted to explain the effect of branch length on DRA performance and stability [12-14]. However, it is important to highlight that there are no adequate experimental studies concerned with the effect of distance between two emitted branches on polymeric DRA performance and mechanical stability. So, the aim of the present investigation is to the synthesis of some polyester series derived from poly(pentaerythritol adipate), poly(pentaerythritol sebacate), and poly(pentaerythritol hexadecandioate), which contain a different number and branch lengths of alkyl groups and assess them as DRA in Iraqi light crude oil as well as evaluate their mechanical stabilities after exposing to a high mechanical shear condition.

2. Materials

Pentaerythritol, sebacic acid, palmitic acid, and calcium chloride (CaCl2) were supplied by Sigma-

Aldrich and used without purification. P-toluene sulfonic acid (pTsOH), also supplied by Sigma-Aldrich, used as a catalyst for the esterification process, was dehydrated before use with toluene using Dean-Stark apparatus to azeotrope off the water at toluene boiling point. Toluene, hexadecandioic acid, and sodium hydroxide supplied by Fluka. The former was firstly dried by calcium chloride, then freshly distilled to obtain dry toluene before use. Adipic acid and Octanoic acid were supplied by BDH and Merch, respectively.

The Iraqi crude oil was supplied by the Zubair field operation division company (ZFOD). Specification of Basrah light crude oil use in the present work is given in Table 1.

Table 1: Physical properties of Iraqi crude oil supplied by ZFOD company

Property	
Viscosity (cSt.) at 35ºC	9
Viscosity (cSt.) at 45ºC	6.5
Viscosity (cSt.) at 55ºC	5.5
Free water (%Vol)	0.02
Emulsion (%Vol)	0
Sediment (%Vol)	0
Bs&W (%Vol)	0.02
Specific gravity at 16ºC	0.870
Specific gravity at 35ºC	0.863
Specific gravity at 45ºC	0.861
Specific gravity at 55ºC	0.858
Asphaltene (%Wt)	2.9
API	31.1
Salt (ppm)	29

3. Methods and experimental work

3.1 Synthesis of 2,2-bis(hydroxymethyl)propane-1,3-diyl dioctanoate

Pentaerythritol (10 g, 1 mol), 1% W/W of pTsOH, and 100 ml of anhydrous toluene were charged into a 500 ml three-neck round bottom flask adopted with Dean-Stark apparatus, quick fitted separatory funnel, and an inlet glass tube for argon gas. Octanoic acid (21.18 g, 2 moles) was added in 100 ml anhydrous toluene and charged into a separatory funnel. Argon gas allows to bubble through the reactant mixture for 5 mins before reaction initiation. Then, the mixture was heated to its boiling point and the octanoic acid solution was added as droplets into the mixture for one hour. The reaction was stopped after one hour of stop water collecting by a graduated tube of Dean-Stark. Next, the mixture was cooled down and washed with water three times to remove pTsOH and the unreacted

pentaerythritol. Finally, the solvent was evaporated using a rotary evaporator and a yellow viscous monomer was obtained. Here some researchers employed pTsOH as a catalyst for esterification reactions [15, 16]. However, the same procedure outlined above was also applied for synthesizing other monomers, namely; 2,2-bis(hydroxymethyl)propane-1,3-diyl dipalmitate and 2,2-bis(hydroxymethyl)propane-1,3-diyl distearate, using 2 moles palmitic acid and 2 moles stearic acid, respectively, instead of octanoic acid, with some considerations were being taken to account and listed in Table 2.

3.2 Synthesis of poly(2,2-bis(hydroxymethyl)propane-1,3-diyl dioctanoate adipate)

M1 (16 g, 1 mole), adipic acid (6.02 g, 1.05 mole), 1% w/w pTsOH, and 200 ml of anhydrous toluene

were placed into 500 ml three-neck round bottom flask fitted with dean-stark apparatus, a glass tube for inlet argon gas and thermometer. The reaction was taken placed at 110oC for 6 hours under argon. Then, the mixture was allowed to cool down to room temperature and 250 ml of 0.01 N aqueous solution of sodium hydroxide was added to extract residual pTsOH and adipic acid. The organic layer was separated and washed with water twice, and then 100 ml of 0.005 N aqueous solution of hydrochloric acid was added. The product was separated, washed with water five times, and finally, evaporated by a rotary evaporator to obtain the yellow waxy product. This procedure was also followed for preparing nine ester polymers by polymerization of 1 mole of each synthesized monomer (M1, M2, and M3) with 1.05 mole of adipic acid, sebacic acid, or hexadecanedioic. Their names, corresponding monomers, and some physical properties are also listed in Table 3.

Table 2: Reaction time, physical appearance, yield percentage, and suggested symbol of synthesized monomers.

Monomer	Corresponding starting materials	Reaction time (h)	Physical apparent	Yield (%)	Symbol
2,2-bis(hydroxymethyl)propane-1,3-diyl dioctanoate	Pentaerythritol, octanoic acid	3.5	Viscous yellow	93.7	M1
2,2-bis(hydroxymethyl)propane-1,3-diyl dipalmitate	Pentaerythritol, palmitic acid	5.5	solid white	92.5	M2
2,2-bis(hydroxymethyl)propane-1,3-diyl distearate	Pentaerythritol, stearic acid	6	solid white	91.2	M3

Table 3: List of prepared polymers with some of their physical-chemical properties.

Monomer or Polymer	Corresponding starting materials	Reaction time (h)	Physical apparent at 25ºC	Yield (%)	Symbol
Poly(2,2-bis(hydroxymethyl)propane-1,3-diyl dioctanoate adipate)	M1 , adipic acid	5	Soft wax yellow	87.3	A1
Poly(2,2-bis(hydroxymethyl)propane-1,3-diyl dioctanoate sebacate)	M1, sebacic acid	6	Soft wax white	85	A2
Poly(2,2-bis(hydroxymethyl)propane-1,3-diyl dioctanoate hexadecanedioate)	M1, hexadecanedioic acid	8	Solid white	85.4	A3
Poly(2,2-bis(hydroxymethyl)propane-1,3-diyl dipalmitate adipate)	M2, adipic acid	7	hard wax yellow	85	A4
Poly(2,2-bis(hydroxymethyl)propane-1,3-diyl dipalmitate sebacate)	M2, sebacic acid	7	hard wax white	83.7	A5
Poly(2,2-bis(hydroxymethyl)propane-1,3-diyl dipalmitate hexadecanedioate)	M2, hexadecanedioic acid	12	Solid white	79	A6
Poly(2,2-bis(hydroxymethyl)propane-1,3-diyl distearate adipate)	M3, adipic acid	7	Solid white	88.1	A7
Poly(2,2-bis(hydroxymethyl)propane-1,3-diyl distearate sebacate)	M3, sebacic acid	10	Solid white to brown	80.6	A8

3.3 Description of circulating flow loop system

Fig. 1 showed the circulating flow system utilized in the current study, which is a fully computerized apparatus made up of (50 × 20 × 10 cm3) controlled temperature tank, horizontal polypropylene pipe

horizontal polypropylene pipe (3 m length, 0.016 m inner-diameter, 0.36 m entrance length and 0.0015 mm internal roughness), 5-150 l/min flowmeter, two pressure transducer sensors, control unit, and two gear pumps; the first one has 100 ml/min maximum flowrate and 1.5 hp, which exert a force on oil to move

into circulating pipe system, the second one has 60 ml/min maximum flowrate and 0.75 hp, was used for transporting oil to inner cylinder rotation system.

3.4 Description of inner cylinder rotation system

Fig. 2 illustrated a schematic diagram of this system which contains two basic components; the variable speed of high torque electric motor of 1 hp and 2900 maximum rpm functionalized by the control circuit and two concentrated cylinders. The inner cylinder, which is shift-connected with the motor, has a dimension of 20 × 5 cm. While the fixed-outer cylinder has a dimension of 25 × 8 cm, acts as an oil chamber.
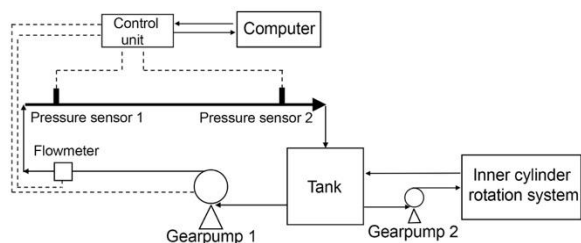
Fig. 1. Schematic drawing of circulating flow loop system.
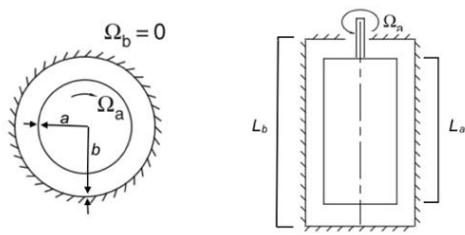
Fig. 2. Inner cylinder rotation system; a is inner cylinder diameter, b is outer cylinder diameter, L_a and L_b are the length of the inner and outer cylinder, respectively.

3.5 Experimental procedure for DRA assessment

The process generally involves adding small quantities of polymers that required to evaluate their performance to the fluid that will be turbulent. Foremost, crude oil (4 L) was charged to the reservoir. To ensure the quick and accurate additions, the DRA stock solution was prepared by dissolving 4 g in 50 ml of crude oil, and then 5 ml, equivalent to 100 ppm, of stock solution was carefully added into the reservoir for each single test. Pre-mixed method was employed at low flowrates of 10-15 l/min for 10 min to ensure adequate mixing for complete dispersal of the polymer solution. In general, testing included automatic and

gradual increasing of crude oil flow rates from 0 to 85 /min at 35°C in 17 incremental steps. Further, each step was kept constant for 5 seconds before data recording to stabilize all sensors. This test was also performed on crude oil before adding DRA doses.

Using critical concentrations of polymers in drag reduction assessments at other temperatures; 45°C and 55°C were also conducted. The crude oil was subjected to a slow heating rate, 0.5°C/min, with continuous circulating oil flow, about 10 l/min. It's worth mentioning that the maximum flow rate was changed at each temperature to maintain a constant Reynolds number range (0-13000).

3.6 Polymer mechanical degradation process

Mechanical degradation of polymer chains was carried out using an inner cylinder rotation system as a degradation device. Polymer-treated crude oil samples were selected where the best drag reduction performance was observed, i.e., polymer critical concentrations. The procedure involved crude oil moving from the reservoir to devise chamber by second gear pump, subjecting of polymer-treated crude oil to large rotational Reynolds number, approximately 23000, using 1000 rpm of rotor speed for 5 min, and eventually, oil gravity drainage to flow loop system reservoir to assess the efficiency of residual polymeric chains. This procedure was applied to each crude oil sample five times in which the final one was extended its degradation period to 10 min.

3.7 Determination of polymer association effect

The number of polymer associations was determined in term of DRA efficiency by using the time-dependence drag reduction experiments which were conducted by recording drop pressure DRA-treated crude oil flow in a time interval of 60 min after exposing to high mechanical shear for once, sufficient to destroy the polymer agglomerations and start polymer degradation, about 23000 rotational Reynolds number for 5 min, i.e. after the first run of polymer degradation assessments.

4. Results and discussion

4.1 FTIR analysis

The reactants and products were characterized by JASCO FTIR 4200 instrument. Similar functional

groups in all partially esterified monomers are typically absorbed within the same frequency ranges. Fig. 3 illustrates the FTIR spectrum of A7, which is compared against its corresponding monomers; M3, pentaerythritol and stearic acid. Analysis of M3 indicates bands absence of carbonyl (C=O) and hydroxyl (O-H) of an acidic group of stearic acid at 1700 cm^{-1} and 2800 cm^{-1}, respectively. More, a remarkable reduction was observed in broadband of pentaerythritol hydroxide group (O-H) at 3400 cm^{-1} and peak of (C-O) at 1037 cm^{-1}. In turn, it indicates the appearance of a new strong band at 1737 cm^{-1} assigned to (C=O) stretching of the new carbonyl ester group. The formation of ester groups was also emphasized by two bands at 1163 cm^{-1} and 1384 cm^{-1} related to (C-O) stretching of the ester group. The presence of both free hydroxyl and ester group in product confirm that pentaerythritol undergoes partial esterification by the nucleophilic attack of hydroxyl groups to the carboxyl acid group of the steric acid. bands between 2850 cm^{-1} and 2950 cm^{-1} refers to existences of (C-H) bond stretching of methyl and methylene groups [17].

Due to the similarity of pattern spectra recorded in all synthesized polymers, the characterization was proceeded by selecting one polymer, A7 for instance, and compared with its corresponding monomer, M3. Broadband absence of free hydroxyl group at 3400 cm^{-1} as well as band reduction of (C-O) bond at 1037 cm^{-1} are the main differences founded in polymer product which imply all free hydroxyl group were consumed in a polymerization reaction by dicarboxylic acid monomer and polymer containing ester linkages in the main chain was finally formed.
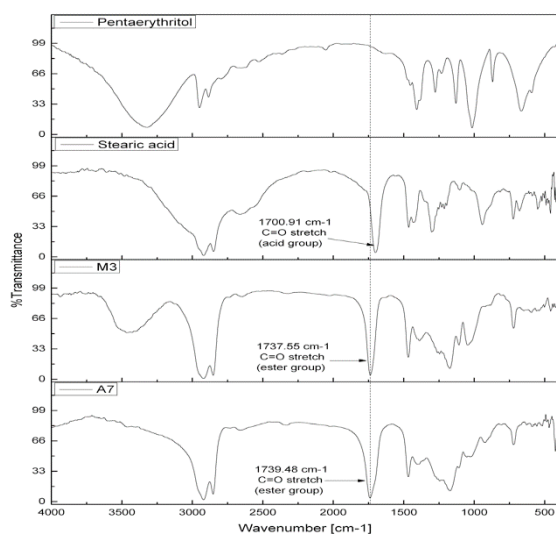

Fig. 3. FTIR of A7 polymer and its corresponding monomer.

4.2 ^{1}H NMR analysis

^{1}H NMR spectres of copolymers were recorded on a Bruker Avance 400 spectrometer at frequency 400 MHz, using CDCl$_3$ as solvent. Fig. 4-6 depict ^{1}H NMR spectrum of polymer products in which all of them indicate appearance of the following signals; at 0.9 ppm related to protons of methyl groups (a) at the end of branches, at 1.4 ppm assigned to neighbour methylene groups protons (b), at 1.7 ppm attribute to methylene group protons (c), at higher chemical shifts of 2.4 ppm belonged to methylene group protons (d), which is a result of electron density deshielding caused by adjacent carbonyl group, and eventually, 4.2 ppm assigned to methylene group protons (e). Protons (e) existed at higher chemical shift which give a good indication of polyester formation where the protons (e) are directly adjacent to oxygen atom of ester group [18]. This evidence is further confirmed by ^{1}H – ^{1}H COSY, 2D NMR technique provides information on coupled spin systems, as shown in Fig. 7. The diagonal signals have been explained and cross signals indicate remarkable correlation of methylene group hydrogen (b) at 1.4 ppm with hydrogen of methylene group (a) and (c), at 0.9 ppm and 1.7 ppm, respectively. An additional correlation was found in hydrogen of methylene group (c), at 1.7 ppm with hydrogen of methylene group (d), at 2.4 ppm. However, protons (e) did not show any correlation.
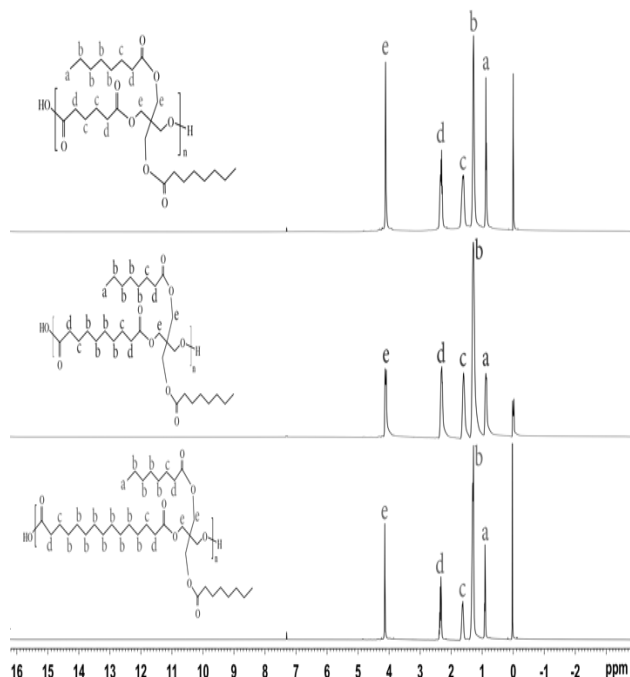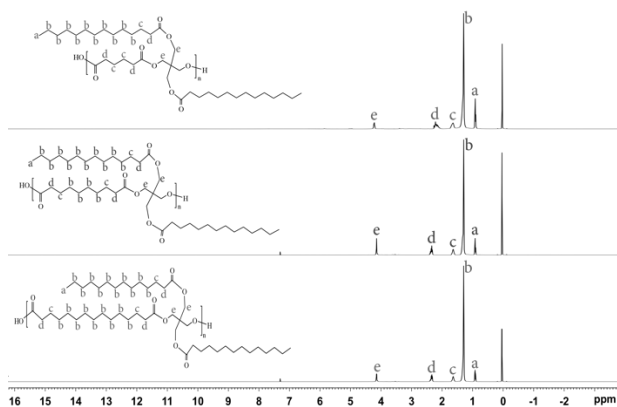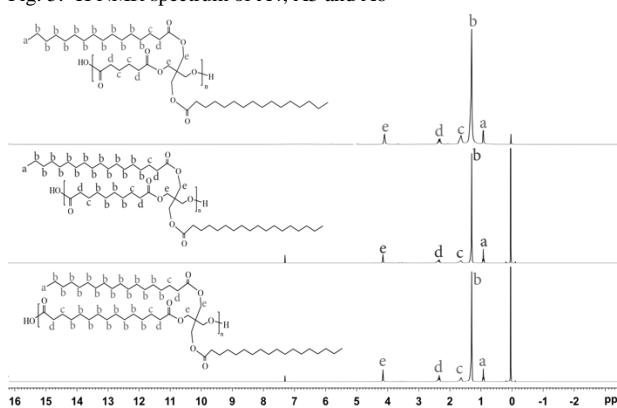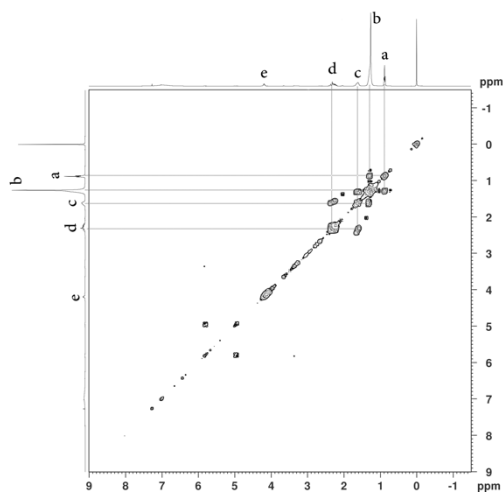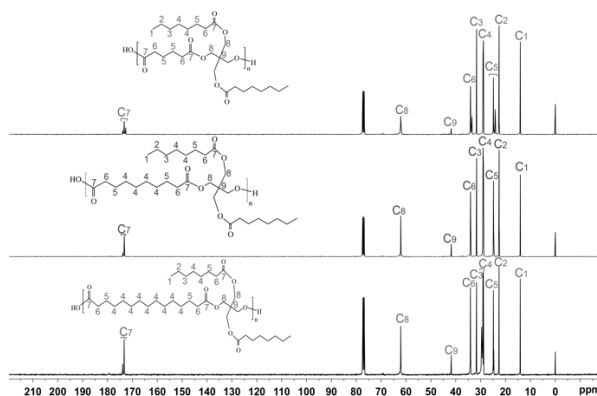

Fig. 4. ^{1}H NMR spectrum of A1, A2 and A3

Fig. 5. ¹H NMR spectrum of A4, A5 and A6

Fig. 6. ¹H NMR spectrum of A7, A8 and A9

Fig. 7.¹H–¹H NMR correlation of A4

4.3 ¹³C NMR analysis

Bruker Avance 400 spectrometer at frequency 100 MHz was also utilized to recorded ¹³C NMR spectra. The solvent was CDCl$_3$ and Fig. 8-10 show ¹³C NMR specters of the present polymers. In ¹³C NMR of A1 polymer, the signal at 15 ppm is corresponding to methyl carbon (C$_1$). While, signals at

22 ppm and 32 ppm were assigned to adjacent methylene carbon (C$_2$) and (C$_3$), respectively. The strong signal at 29 ppm was related to the carbon (C$_4$) of methylene group constituted midsection of branches. The environment of carbonyl carbon (C$_7$) shows deshielded signal at 174 ppm and signals at 34 ppm and 24 ppm were attributed to nearby methylene carbons (C$_5$) and (C$_6$), respectively. The signal of quaternary carbon (C$_9$) was located at 42 ppm [19].

The signal at 62 ppm may attributed to the formation of polyester, which assigned to carbon (C$_8$) of methylene group, nearby oxygen of ester group. The electron withdrawing of oxygen of ester groups is shifted the adjacent carbon atom through reducing amount of electron density around it leads to emergence ¹³C NMR signal at higher ppm [20]. This outline is basically the same as that in other polymers, A2-A9, with one remarkable difference was found in signal intensity of methylene carbon (C$_4$), 29 ppm, which appeared considerable as the longer alkyl branches or longer distances between branch points exist in polymer structure.

Fig. 8. ¹³C NMR spectrum of A1, A2, and A3
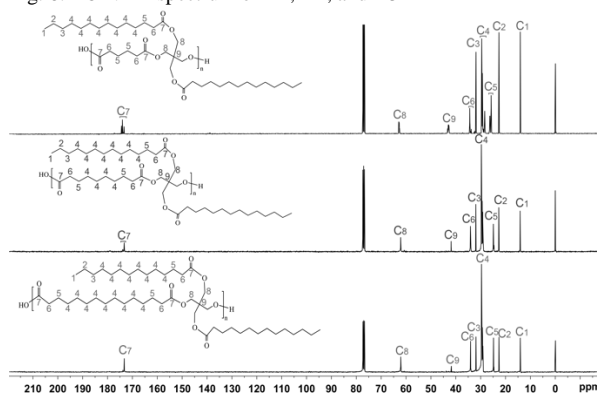
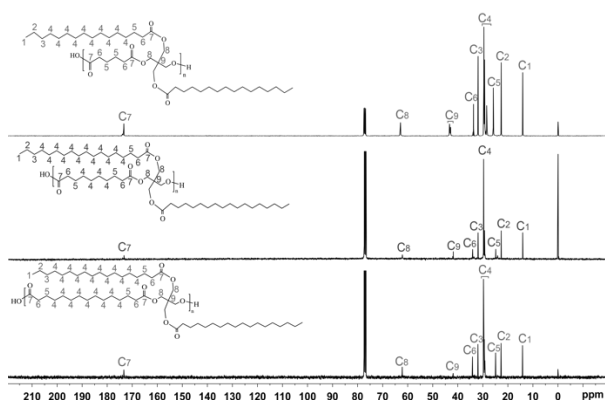Fig. 9. ¹³C NMR spectrum of A4, A5, and A6

Fig. 10. ^{13}C NMR spectrum of A7, A8, and A9

4.4 Determination of polymers molecular weight

The number-averages molecular weights of synthesized polymers were determined by the group acid analysis method (ASTM D1386 – 98) [21]. The results, stated in Table 4, reveal that the molecular weights of polymers are almost comparable and the relative decline in the number of repeating units is the monomers molecular weights dependent in which polymerizing few numbers of large-sized monomers can provide chains with enough steric hindrance that difficult to reacting with another chains [22].

Table 4: Molecular weights and number of repeating units of ester polymers in the present study.

Polymer	Mn	No. of repeating units
A1	27400	54.9
A2	22170	40.01
A3	22390	35.88
A4	26760	40.18
A5	25100	34.71
A6	24300	30.64
A7	27430	37.95
A8	25010	29.95
A9	27080	29.88

4.5 Effect of polymeric DRA concentration

The relationship between the drag reduction percentage and the volumetric flow rate of crude oil in terms of Reynolds was depicted in Fig. 11-19. Modification of turbulence flow was carried out by presenting polymer in minute concentrations, ranged from 100 up to 700 ppm, in the crude oil at 35oC. All polymers were demonstrated suppression ability to eddies at higher Reynolds numbers. The positive effect of flow rate on DRA performance was well-identified in many kinds of literature due to increase turbulence and thus, the polymer is induced to undergo a coil-to-stretch at higher transition rates [23]. All tested

polymers showed noticeable improvement in reducing pressure drop by increasing their concentrations. This phenomenon was clarified by the elastic sub-layer model theory of Virk [24]. However, after a certain dose of DRA, level-off drag reduction was presented and, on the basis of this information, both the critical concentration (Cmax) and the maximum drag reduction were then determined. Table 5 summarized The drag reduction measurements of polymers at 12000 Reynold number and 35oC.

Although the number average molecular weights of prepared polymers are nearly comparable, there is a fluctuation in that DRA compatibility due to change in side chain length as well as the distance between side chains, and consequently, variation in the polymer-solvent interaction [25]. It was baffling that both A1 (short length side chains and the short distance between branch points) and A9 (long length side chains and long-distance between branch points) are more efficient in turbulent flow, about 38%, and 37% drag reduction percentage when using 700 ppm and 400 ppm, respectively. However, the main difference was found in their critical concentrations. Polymers containing longer side chains showed better performance than the shorter ones. This is due to longer branches that can impart polymer hydrocarbon solubility and, for this reason, better polymer-solvent interaction and drag reduction properties [26]. A1 required 700 ppm to reach the maximum drag reduction percentage while 600 ppm for both A4 and A7. Likewise, it takes 500 ppm for A3 and A6, and 400 ppm for A9.

The effect of distance between two branch points was also investigated and showed a significate impact on Cmax. Polymer chains containing adipic acid segment as main part constituted backbone A1, A4, and A7, are required concentrations more than other analogous polymers containing sebacic acid or hexadecandioic acid segments to achieve Cmax. Also found that polymer backbone manipulation can be considered important in Cmax decreasing rather than the length of the side chain. Fig. 20 shows how a change in Cmax could affect when adding ten methylene groups, ones in the backbone A3 and others in branches chains A7. Another observation involves reaching maximum drag reduction at lower flow rates as the distance between two side chains is increased. This effect is obvious in A9 in which the maximum drag reduction was level off about 1300 Reynolds number less than A7.
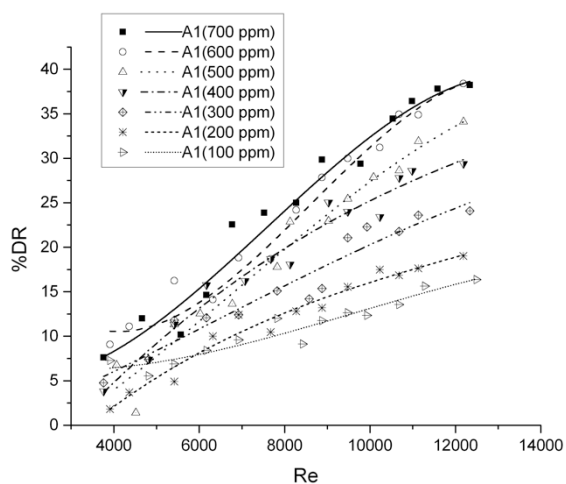
Fig. 11. %DR vs. Reynolds number for different concentration of polymer A1 at 35ºC
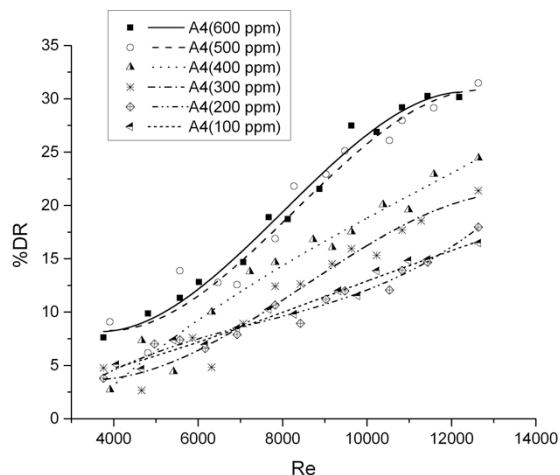

Fig. 14. %DR vs. Reynolds number for different concentration of polymer A4 at 35ºC
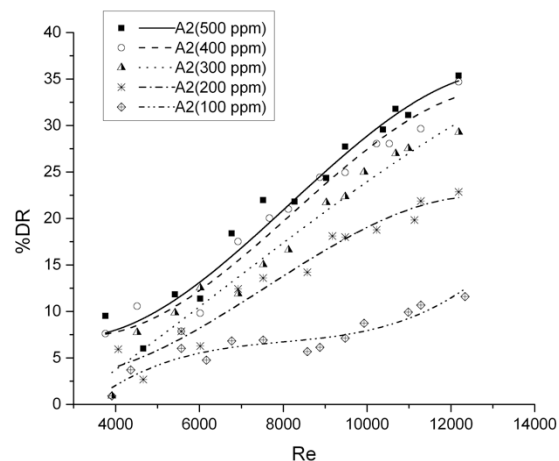

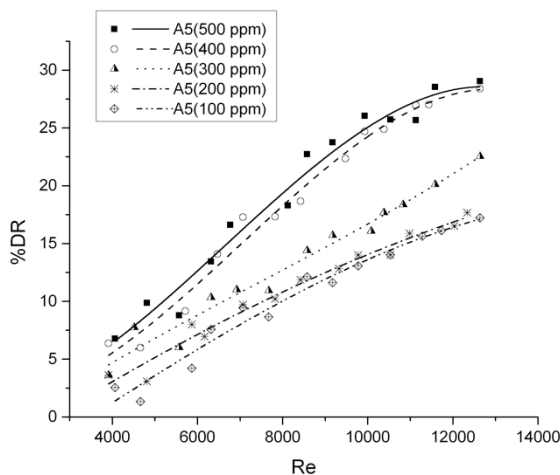Fig. 12. %DR vs. Reynolds number for different concentration of polymer A2 at 35ºC

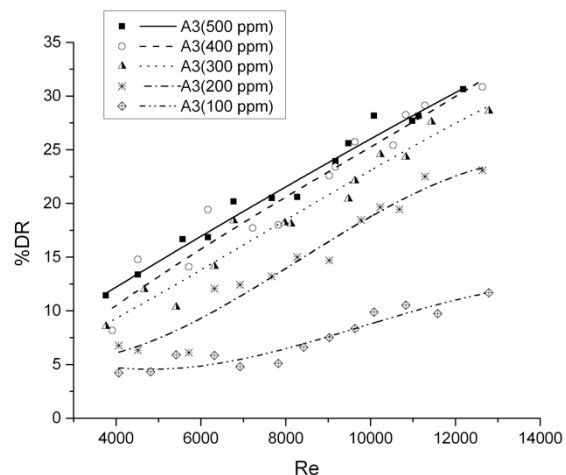Fig. 15. %DR vs. Reynolds number for different concentration of polymer A5 at 35ºC

Fig. 13. %DR vs. Reynolds number for different concentration of polymer A3 at 35ºC

Fig. 16. %DR vs. Reynolds number for different concentration of polymer A6 at 35ºC

Fig. 17. %DR vs. Reynolds number for different concentration of polymer A7 at 35°C
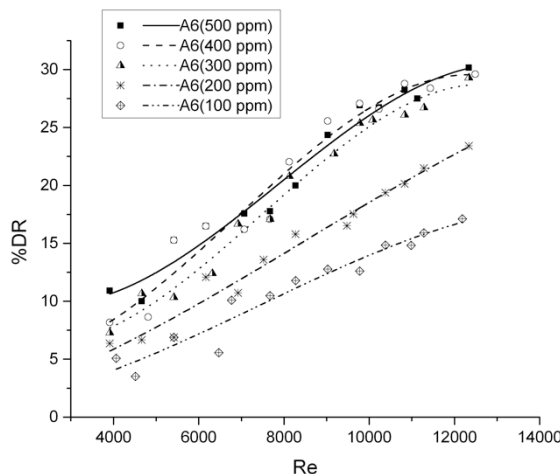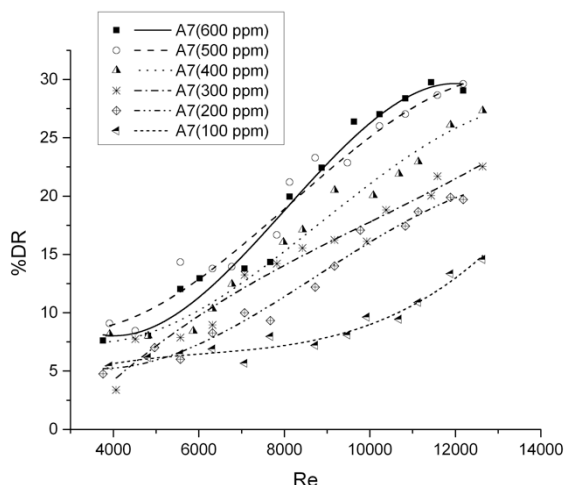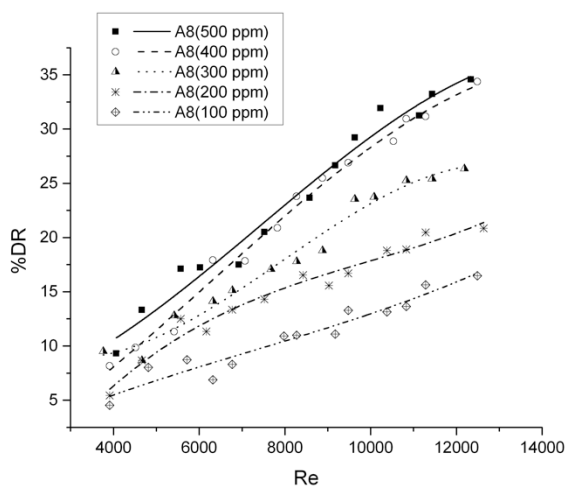

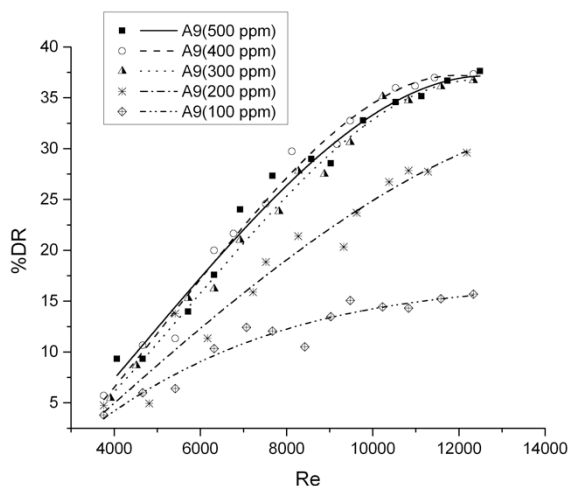Fig. 18. %DR vs. Reynolds number for different concentration of polymer A8 at 35°C

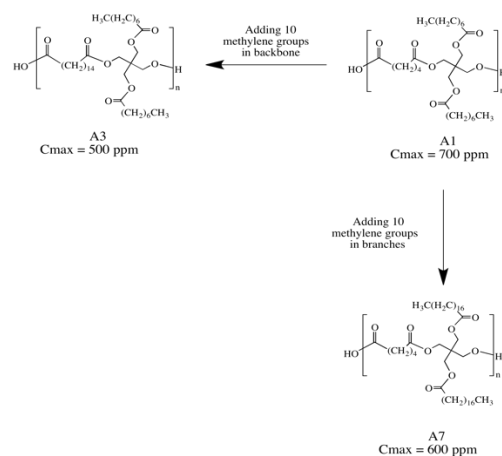Fig. 19. %DR vs. Reynolds number for different concentration of polymer A8 at 35°C

Fig. 20. Effect of adding ten methylene groups to polymer structure on Cmax.

Table 5: List of %DR and C_{max} and tested polymers at 35°C and 12000 Reynolds number

DRA	C_{max} (ppm)	$\%DR_{max}$
A1	700	38%
A2	500	34.8%
A3	500	30.5%
A4	600	30.1%
A5	500	28.5%
A6	400	29.1%
A7	600	29.5%
A8	500	34%
A9	400	37%

4.5 Effect of temperature

Plotting the maximum drag reduction of tested polymers at their critical concertation and 12000 Reynolds number as a function of the temperature as depicted in Fig. 21. It was found that increasing the temperature leads to decreasing in the drag reduction efficiently for most of the tested polymers. Nevertheless, this effect considerably varies and is predominantly found in polymers having the adipic acid segment as a part of backbone chains (A1, A4, and A7). About 2% of drag reduction efficiency was decreased in A1 polymer at 45°C, compared to the same DRA performance at 35°C, and much lower drag reduction at 55°C, about 6%. However, other polymers with hexadecandioic acid segments are found to be more thermally sustainable polymers against elevated temperatures. For example, only 1% DRA effectiveness of A9 was reduced when the temperature changed from 35°C to 55°C.
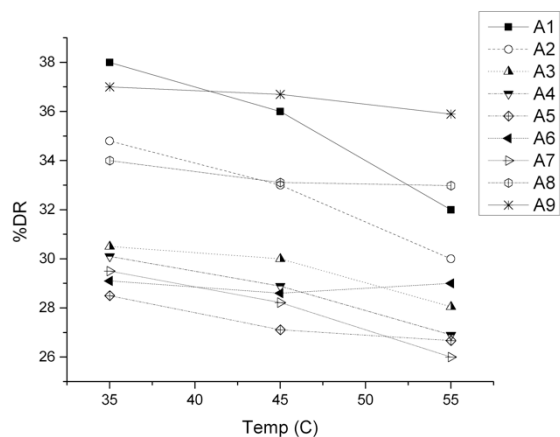
Fig. 21. Temperature effect on %DR of tested polymers at their Cmax and 12000 Reynolds number

4.6 Evaluation of polymer mechanical stability

Fig. 22 compares the DRA efficiency at 12000 Reynolds number and at 35°C between polymers A1, A4, and A7, containing adipic acid segment as a complementary part of the repeating unit. Although a high concentration of A1 polymer was used to achieve a maximum drag reduction of 38%, it also showed lower durable and resistance to mechanical degradation among other tested polymers, about 65.79% of %IE was rapidly decreased after 20 min of shear degradation, and 68.95% after 30 min. the longer side chain can appreciably enhance polymer mechanical stability, around 55.93% and 56.18% of %IE were dropped for A4 and A7 after 30 min under 23000 rotational Reynolds number, respectively. Similar behaviors were observed in other polymers having larger distances between branches points, as shown in Fig. 23 and Fig. 24, in which A8 and A9 significantly demonstrated more resistance to degradation, about 50% and 62.16% of %IE, respectively, remain after 30 min of exposing to mechanical shear.

Two major reasons can be suggested to explain and to justify this imbalance; As polymers have almost the same range of molecular weight, the number of ester groups per unit volume is dramatically decreased from A1 to A9 and this has been also matched by increased the amount of methylene group constituted polymer structure. This modification can increase polymer hydrocarbon solubility and thus, the polymer adopts a random coil (expanded conformation) instead of globular conformation [27]. Nakano and Minouta [28] pointed that the dependence of mechanical

degradation rate of polymer on solvent through altering the expansion degree of polymer chains in which applied shear force is more effective on folded or contracted polymer chain than an expanded one. Similar results are found in other studies [29, 30]. More, esters are polar groups and a large number of polar groups leads to coils shrinks, tend to agglomerate with each other in a poor solvent, and forming associations by hydrogen bondings which can easily break down when a high shear force is applied [31, 32] and, consequently, noticeable decreasing in %IE of A1 at first stages of mechanical degradation.

As polymer agglomeration was relevant here, time dependence – agglomeration assessment was also conducted and the results, shown in Table 6, provide further confirmation that polymers containing shorter branches length and shorter distance branch points can re-aggregated after a certain time of interval. The recovering of %IE was mainly found in A1, about 15.13%, and a minimal presence in A9, about 2.65% after 60 min of the time interval. In this regard, the high drag reduction efficiency, high critical concentration, and negative temperature dependence of A1 and similar polymers can be explained by week associations presenting between polymer chains [33-35]. This effect was significantly decreased by an increasing distance between branches and seen when presenting hexadecandioc acid in the polymer backbone.
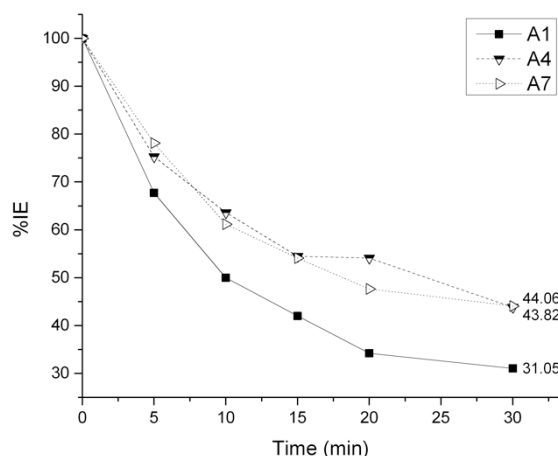

Fig. 22. Time-dependence of drag reduction efficiency A1, A4, and A7 polymers after exposing to 30 mins of shear, tested at their Cmax, 35°C, 12000 Reynolds number.

Fig. 23. Time-dependence of drag reduction efficiency A2, A5, and A8 polymers after exposing to 30 mins of shear, tested at their Cmax, 35°C, 12000 Reynolds number.
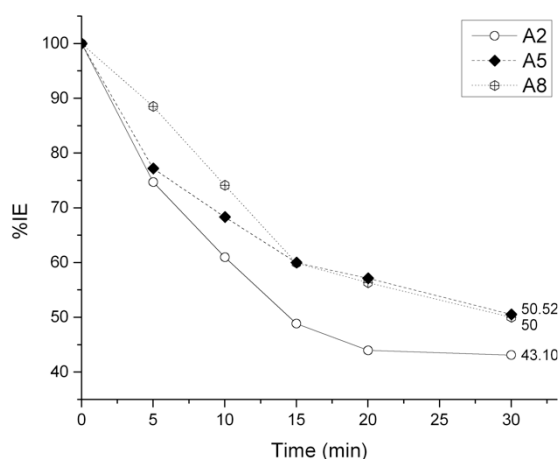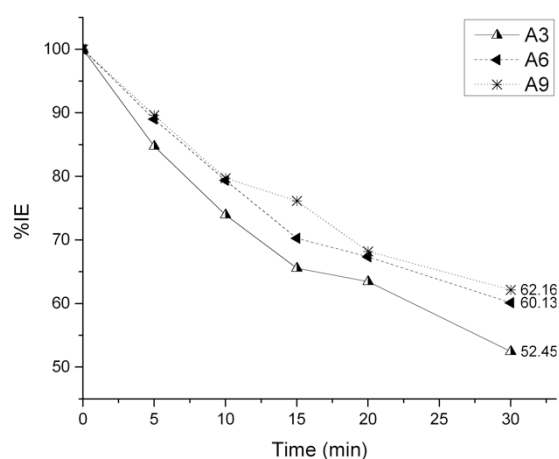

Fig. 24. Time-dependence of drag reduction efficiency A3, A6, and A9 polymers after exposing to 30 mins of shear, tested at their Cmax, 35°C, 12000 Reynolds number.

Table 6: Influence of chemical structure on recovered efficacy, △IE is differential efficiency after 60 min of time interval at 35°C and Reynolds number of 12000

Polymer	No. of ester Carbons incorporated one branch	No. of diester Carbons incorporated polymer backbone	△%IE
A1	8	6	15.13%
A2	8	10	13.47%
A3	8	16	5.94%
A4	16	6	10.63%
A5	16	10	9.48%
A6	16	16	5.85%
A7	18	6	6.27%
A8	18	10	4.12%
A9	18	16	2.65%

5. Conclusion

In summary, a successful strategy was implemented for providing a broader perspective on the effect of branch lengths as well as the distance between branch points on polymeric DRA performance in Basrah crude oil samples using a flow loop circulation system. It was found that some of the tested polyesters were considered to be within the effective drag reduction agent category. Poly(2,2-bis(hydroxymethyl)propane-1,3-diyl dioctanoate adipate) and Poly(2,2-bis(hydroxymethyl)propane-1,3-diyl distearate hexadecanedioate) are more efficient than analogous polymers and the maximum drag reduction achieved was 38% and 37% using concentrations of 700 ppm and 400 ppm, respectively, at 35°C and 12000 Reynolds number. Moreover, it was concluded that the space between two branch points is as an important factor as branch length on critical concentration where both of them have contributed to decreasing the critical concentration of polymer, with the better results goes to the former. Ester groups are also found to have a potential effect only in the enhancement of drag reduction performance through providing week intermolecular forces induce polymer chains to aggregate and increase the apparent molecular size of DRA. The temperature dependence and degradation experiments were also reported here. It was revealed that weak intermolecular forces via ester groups have a short term destructive effect on polymer mechanical stability and a negative impact on DRA performance with increasing temperature. A longer distance between branch points, as much as C_{16}, makes polymer in a higher level of methylene content and lower number of the ester groups which reflects its improvement on DRA performance at elevated temperature, better mechanical stability, and lower doses of polymer used.

6. References

[1] Hart A., A review of technologies for transporting heavy crude oil and bitumen via pipelines. *The Journal of petroleum exploration and production technology*, **4**, 327-336 (2014).

[2] Toms. B. A., Some observation on the flow of the linear polymer solution through straight tube at large Reynolds numbers, In *proceeding of the 1st international congress on rheology*, **2**, 135-141 (1948).

[3] Burger E. D., Munk W. R. and Wahl H. A., Flow increase in the Trans Alaska pipeline through use of a polymeric drag-reducing additive. *Journal of petroleum technology*; **34**(2), 377-386 (1982).

[4] Rabeeah H. S., Abduallah A. B. and Sultan O. M., Improvement of Sharara crude oil flow using

polystyrene and polydimethylsiloxane as drag reducing agents. *Journal of applied science*, **2**(1), 14-28 (2019).

[5] Cole D. P., Khosravi E. and Musa O. M., Efficient water-soluble drag reducing star polymers with improved mechanical stability. *Journal of polymer science, part A : polymer chemistry*, **54** (3), 335-344 (2016).

[6] Xing L., Ke Y., Hu X.and Laing P., Preparation and solution properties of polyacrylamide-based silica nanocomposites for drag reduction application. *New journal of chemistry*, **44**(23), 9802-9812 (2020).

[7] Xianwu J., Youquan L., wei L., Yuan X. and Zhiyu H., Using water-miscible nonionic hydrophobic monomer associating HPAM as drag reducing agent. *Journal of applied polymer science*, **136**(48), 48362 (2019).

[8] Guoyan M., Xiaorui L., Xiaorong W., Guanjun L., Luan J. and Kia Y., Preparation, rheological and drag reduction properties of hyrophobically associating polyacrylamide polymer. *Journal of dispersion science and technology*, **40**(2), 171-179 (2019).

[9] Huang W., *M.Sc. thesis*, University of Waterloo, Canada (2015).

[10] Bari H. A. and Faraj E., Studying the interaction between a new mixture in enhancing drag reduction efficiency. *International Journal of Chemical Engineering and Applications*, **4**(4), 277-280 (2015).

[11] Dai X., Li G., Li J., Xin Y., Yang G. and Zhang Y., Potential of surfactant as anti-shear additive for DRA of oil", *2nd International Workshop on Materials Engineering and Computer Sciences (IWMECS)*, Chongqing, China, 370-373 (2015).

[12] Bae Z, Milligan S. N., Olechnowicz M., Johnston R. L., Burden T. L., Smith K. W., Harris W. F. and Dreher W. R, US patent 9784414 B2 (2017).

[13] Tavtorkin A. N., Gavrilenko I. F., Kostitsyna N. N., Korchagina S. A. and Chinova M. S., Comparison of the turbulent drag reduction effectiveness of polymers from higher olefin monomers (hexane, octane, decene, dodecene) in the production of hydrodynamic drag reducing agent for transportation of hydrocarbon liquids. *Russian journal of applied chemistry*, **93**(6), 788-793 (2020).

[14] Brostow W.and Lobland H. E. H., Lowering mechanical degradation of drag reducers in turbulent flow. *Journal of material research*, **22**(1), 56-60 (2006).

[15] Ananda A. S., Uyen H. and Nnaemeka O. C., Renewable polymers: Synthesis and characterization of poly(levulinic acid-pentaerythritol). *Journal of polymer science*, **56**(9), 955-958 (2018).

[16] Sun L., Zhu L., Weilan X. and Zeng Z., Kinetic of p-toluene-sulfonic acid catalyzed direct esterification of pentaerythritol with acrylic acid for pentaerythritol diacrylate production. *Chemical engineering communications*, (**207**)3, 331-338 (2020).

[17] Silverstien R. M., Webster F. X. and Kiemle D. J., "Spectrometric identification of organic compounds",8th Ed., Joun Wiley & Sons Inc., New York (2014).

[18] Thomas J.and Bruno D. N. P., "Handbook of basic table for chemical analysis", 4th Ed., CRC Press- LLC, USA (2020).

[19] Di Pietro M. E., Mannu A. and Mele A., NMR determination of free fatty acids in vegetable oils. *Processes,* **8**(4), 410 (2020).

[20] Šarića A., Gotića M., Štefanića G.and Dražić G., Synthesis of ZnO particles using water molecules generated in esterification reaction. *Journal of molecular structure*, **1140**, 12-18 (2016).

[21] ASTM Standard D1386 – 98, *Standard test method for acid number (empirical) of synthetic and natural waxes", 100 Barr harbor drive, West Conshohocken, PA 19428-2959*, United States (1998).

[22] Odian G., "Principle of polymerization", 4th Ed, John Wiley & Sons, Inc., US (2004).

[23] Larson R. G. and Magda J. J., Coil-stretch transitions in mixed shear and extensional flows of dilute polymer solutions. *Macromolecules*, **22**(7), 3004-3010 (1989).

[24] Virk P. S., Merrill E. W., Mickley H. S. and Smith K. A., The Toms phenomenon: turbulent pipe flow of dilute polymer solutions. *Journal of fluid mechanics*, **30**(2), 305-328 (1967).

[25] McCormick C. L., Hester R. D., Morgan S. E. and Safieddine A. M., Effect of molecular structure on drag reduction efficiency. *Macromolecules*, **23**(8), 2124-2131 (1990).

[26] Kim C. A., Choi H. J., Sung J. H., Lee H. M. and Jhon M. S., Effect of solubility parameter of polymer-solvent pair on turbulent drag reduction. *Macromolecular Symposia*, **222**(1),169-174 (2005).

[27] Luna-Barcenas G., Meredith J. C., Sanchez I. C. and Johnston K. P., Relationship between polymer chain conformation and phase boundaries in a supercritical fluid. *The journal of chemical physics*, **107**(24), 10782-10792 (1997).

[28] Nakano A. and Minoura Y., Effect of solvents on the degradation of polymer by high-speed stirring. *Journal of applied polymer science*, **16**(3), pp:627-643 (1972).

[29] Hunston D. L. and Zakin J. L., Flow-assisted degradation in dilute polystyrene solution. *Polymer engineering and science*, 20(7), 517-532 (1980).

[30] Brostow W., Macip M. A. and Sochanski J. S., Macromolecular conformations in solutions. II. Thermodynamics of interactions. *Journal of statistical physics*, 29(4), 865-878 (1982).

[31] Fumihiko T. and Tsuyoshi K., Temperature-responsive polymers in mixed solvents: Competitive hydrogen bonds cause cononsolvency. *Physical review letters*, **101**(2), 028302 (2008).

_____

[32] Debashish M., Carlos M. M., Torsten S. and Kurt K., Depleted depletion drives polymer swelling in poor solvent mixtures. *Nature communications*, **8**, 1374 (2017).

[33] Shetty A. M. and Solomon M. J., Aggregation in dilute solutions of high molar mass poly(ethylene) oxide and its effect on polymer turbulent drag reduction. *Polymer*, **50**(1), 261–270 (2009).

[34] Coelho E. C., Barbosa K. C. O., Soares E. J., Siqueira R. N. and Freitas J. C. C., Okra as a drag reducer for high Reynolds numbers water flows. *Rheologica Acta*, **55**, 983–99 (2016).

[35] Maki Y., Chain collapse and aggregation in dilute solutions of poly(methyl methacrylate) below the theta temperature. *Polymer journal*, **46**, 641-645 (2014).

_____

الملخص العربي

تأثير التباين في بنية البوليمر على قمع دوامات متكونه خلال التدفق المضطرب للنفط الخام البصرة الخفيف

ماهر اسعد جلال¹, مؤيد نعيم خلف² ومؤيد عبد العال حسين²

١. قسم كيمياء وتكنولوجيا البوليمرات، مركز ابحاث البوليمر، جامعة البصرة، البصرة، العراق

٢. قسم الكيمياء، كليه العلوم، جامعه البصرة، البصرة، العراق

تضمنت الدراسة تحضير مشتقات البولي(اديبات بنتااريثريتول) والبولي(سيبايات بنتااريثريتول) والبولي(هيكساديكاندايوات بنتااريثريتول)التي تحتوي على فروع ألكيلة مختلفة الاطول بخطوتين متتاليتين ؛ تفاعل خماسي الإريثريتول مع الأحماض الأليفاتية أحادية الكربوكسيل الخطية التي تحتوي على ، باستخدام ذرات الكاربون من ٨ الى ١٦ ثم بلمرة المنتجات باستخدام أحماض أليفاتية ثنائية الكربوكسيل التي تحتوي على ذرات كاربون من ٦ الى ١٦ ١٪ بارا التولوين حمض السلفونيك كمحفز. تم تنقية المنتجات وشخصت بواسطة مطيافيه الأشعة تحت الحمراء والرنين النووي المغناطيسي. كما تم استخدام تحليل المجموعة النهائية كطريقة لتحديد الوزن الجزيئي. تمت دراسة خصائص هذه البوليمرات في تقليل الاضطراب الحاصل خلال التدفق النفط الخام الخفيف للبصرة باستخدام نظام الدوران مغلق للنفط. وجد أن بعض البوليمرات يعمل بشكل جيد في تقليل الاضطراب الحاصل للنفط خلال عمليه المتدفق ووجد أيضا أن فعالية البوليمر تعتمد على تركيزه وتركيبه الكيميائي وعلى معدل التدفق ودرجة الحرارة النفط المستخدم. وكما تم دراسة تأثير القص الميكانيكي المطبق على البوليمر كدالة للوقت باستخدام جهاز دوار أسطواني ووجد أن المسافة بين نقاط التفرع للسلسلة البوليميرية تلعب دورًا مباشرًا في المساهمة في أداء البوليمر واستقراره الميكانيكي

_____